Static compaction in laboratory of treated fine soils

Jean-Francois Serratrice

Static compaction in laboratory of treated fine soils

Jean-François Serratrice
Cerema Méditerranée, Aix en Provence, France

Contact: jean-francois.serratrice@cerema.fr

Abstract

A static compaction method is used to prepare specimens for mechanical laboratory tests on untreated or treated fine soils. The method has been enhanced with the record of the curves giving the compaction force as a function of the soil settlement. The compaction procedure is described. The properties of the soils tested are listed. Examples of static compression curves are shown and commented on. The parameters identified on these curves are related to the soil properties. Trends are discussed. The effects of the treatments are examined.

Keywords: static compaction; treated fine soils; compaction curve; laboratory tests.

1 Introduction

Soil compaction plays a central role in the construction of earthworks for practical and economic reasons. The soil obtained from the field is initially destructured and then densified to offer specific mechanical and hydraulic characteristics within the fill. Treatment with hydraulic or other binders aims to improve the properties of the compacted soil. Soil treatment and compaction are carried out by applying rules based on practice and translated into standards [1].

In the laboratory, the mechanical properties such as deformability and shear strength or the hydraulic properties of untreated or treated compacted soils are collected by means of oedometer tests or triaxial tests. In order to carry out these tests, it is necessary to compact specimens whose responses must be as representative as possible of the behaviour of the compacted soil in the fill. Dynamic compaction, Proctor type or derived, is used to reconstitute these specimens [2] [3]. But static compaction is favoured for its sensitivity and ability to provide homogeneous specimens with good repeatability [4] [5] [6] [7].

This study presents experimental data collected during static compaction of specimens for mechanical testing. Densification of the wet soil is carried out by compression in a mould using the method recommended by [5]. The method has been enhanced with the logging of the curve that links compressive load to soil settlement, considering that compaction provides the mechanical history of the compacted soil before it is subjected to mechanical tests [8].

In this study, attention is drawn to fine soils treated with different types of binders (road binders, clay, sand). The paper starts with the description of the static compaction method, followed by the presentation of the soils tested and their physical properties. Examples of static compression curves are shown for untreated and treated soils. Then, the compressibility parameters, which describe the densification of the initially bulked soils, are identified on these experimental curves. The main trends observed are commented on.

2 Test method, soils tested

2.1 Static compaction

The method for preparing oedometric or triaxial test specimens includes the following stages: preparation of the soil and possible treatment, static compaction, demoulding and possible conservation. The specimens are then placed in the test cells. They are saturated or not, depending on the purposes of the tests, before being processed through the mechanical test procedure.

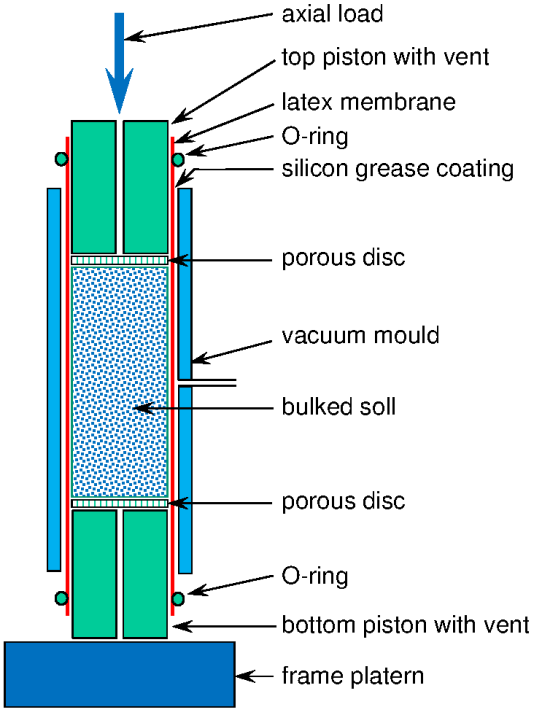

Figure 1. Diagram of the static compaction mould

The state of the compacted soil, the target of static compaction, is defined by a water content and a dry density (w_0, ρ_{d0}) or a water content and a void ratio (w_0, e_0). Most often, these specifications refer to the normal Proctor optimum of the compacted soil (water content w_{OPN} and dry density ρ_{dOPN}).

The method is applicable to fine soils containing less than 5% of particles larger than 2 mm in diameter which can be removed by sieving. The soil is first destructured and air-dried. The next step is to moisten the soil to bring its initial water content w to the target w_0 ($w < w_0$ in most cases). To produce a homogeneous moistened soil, a preparation method without mixing was proposed by [9]. The required soil mass is spread on a plate carried by a balance and then moistened by spraying water until the desired wet mass is reached. The moistened soil is placed in a tightly sealed transparent bag and stored for at least 24 hours for water moisture equilibration. When the soil is treated, the binder is incorporated into the moistened soil immediately before static compaction (no delay in compaction) and is thus integrated into the densification process.

The triaxial specimens have a target slenderness of two. They are prepared in a steel mould of 50 mm internal diameter and 250 mm height (Figure 1). The final target height is therefore 100 mm. To reduce the lateral friction of the soil on the mould wall, the mould is greased and coated with a latex membrane. The humidified soil is introduced into the mould where it occupies the height h_0. Compaction is carried out between these two floating pistons using a compression frame at a rate of about 5 mm/min, i.e. for a period of 20 to 30 minutes. At this rate, a quasi-stabilised compaction can be achieved at each stage of compaction. The advantage of this method is that it produces a triaxial specimen in a single phase, while ensuring good homogeneity of the compacted soil. The oedometer specimens are compacted directly in the test cell following a similar procedure.

The quasi-continuous loading of the bulked soil is carried out in small successive steps during which the axial force F indicated by a dynamometer ring and the settlement Δh measured with a stainless steel rule are recorded. The loading is increased until the target height of the compacted specimen is reached, plus a small additional loading to allow for the swelling to be expected during unloading.

2.2 Characterisation of compaction curves

By recording the settlement Δh and the compressive load F, the variation of the void ratio e, or the axial deformation ε_a, can be described as a function of the total axial compaction stress σ_a ($\varepsilon_a = \Delta h/h_0$, $e = e0 - (1+e_0)\,\varepsilon_a$, $\sigma_a = F/A$, A mould cross-section area). Thus, static compaction is expressed using the three main variables: water content w, void ratio e (or ρ_d) and total axial stress σ_a. The plane ($\log(\sigma_a)$, e), where the compressibility of the soil is observed, is associated with the state plane (w, e).

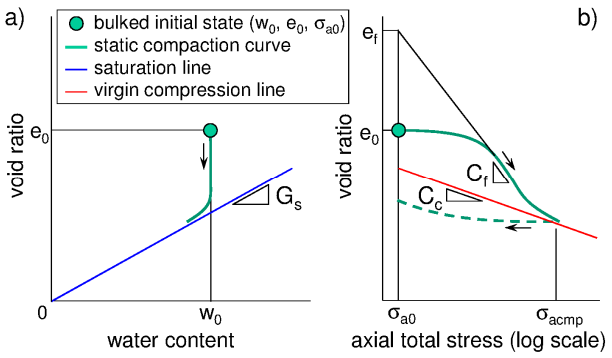

Figure 2. Static compaction curve; a) In the state plane (w, e); b) In the compressibility plane ($\log(\sigma_a)$, e)

In the (w, e) plane, the iso-degree of saturation curves are straight lines of equation $e = (w\,\rho_s)/(S_r\,\rho_w)$ where ρ_s is the unit weight of the solid particles, ρ_w is the unit weight of the water and S_r is the degree of saturation. The equation is also written $S_r\,e = w\,G_s$ where $G_s = \rho_s/\rho_w$ is the density of the solid particles. In particular, the saturation line has the equation $e = G_s\,w$ ($S_r = 1$), Figure 2a.

The compaction path takes place at constant water content $w = w_0$, until a state close to the saturation line is reached. The minimum void ratio that can be achieved is $e_{inf} = w_0\,G_s/S_{rinf}$ where the degree of saturation S_{rinf} is close to unity. A higher density ($e < e_{inf}$) can only be achieved if soil drainage is possible, by extending the loading duration and increasing the axial load.

Figure 2b shows the compression curve ($\log(\sigma_a)$, e) of the bulked soil, from its initial state (σ_{a0}, e_0) to the maximum axial stress σ_{amax} that needs to be applied to reach the target compacted state ($\sigma_{a0} = 1$ kPa is the unit axial stress). The static compression curve is followed by the unloading curve (dotted line). The graph also shows the compressibility line of the saturated reconstitued soil with slope C_c (virgin curve). This line can be obtained after mixing the soil at high water content, followed by a stepwise oedometric compression. The static compression curve lies above the virgin compression line. It can be characterised by the maximum slope $C_f = \max[\Delta e/\Delta\log(\sigma_a)]$ and its ordinate e_f. The maximum axial stress σ_{acmp} is the abscissa of the point where the compaction curve joins the virgin line. The parameters e_f and C_f are identified on the static compression curves. These parameters are examined in the following analysis.

2.3 Soils studied

The data analysed in this study were collected from about 50 soils that were compacted in the laboratory for triaxial and oedometer tests (monotonic and cyclic tests, permeability, shrink and swell tests). The majority of the soils tested are fine silty and clayed soils. Some soils were sandy. A few were taken from existing embankments.

From this data set, six examples are presented here. The physical properties of the soils are reported in Table 1 (C_2 particle size less than 2 µm, V_B methylene blue value). The normal Proctor optimum is then given. According to the classification of fine soils [1], the soils fall into the subclass F1, F2 and F3 of fine soils with low, medium and high plasticity. Two of these soils are selected in the following to present the static compression curves of clayed soils (lines 1 and 2). The other four soils are treated in different ways (lines 3 to 6).

Table 1. Physical properties of the soils studied

Sol	ρ_s (g/cm^3)	w_L (-)	I_p (-)	C_2 (%)	V_B (g/100g)	w_{OPN} (%)	ρ_{dOPN} (g/cm^3)	Class
Goderville silt	2.67	41	19	35	3.5	17.0	1.75	F2
Bavent clay	2.77	46-53	23-28	35	4.1	19.6	1.71	F3
Clayed marl	2.70	70	32	-	-	26.7	1.50	F3
Plastic clay	2.51	66	36	47	-	15.8	1.61	F3
Weathered marl	2.65	-	-	-	3.3	15.3	1.83	F2
Sandy loam	2.75	31	9	12	0.9	12.3	1.95	F1

3 Examples for untreated soils

3.1 Example of a clayey silt

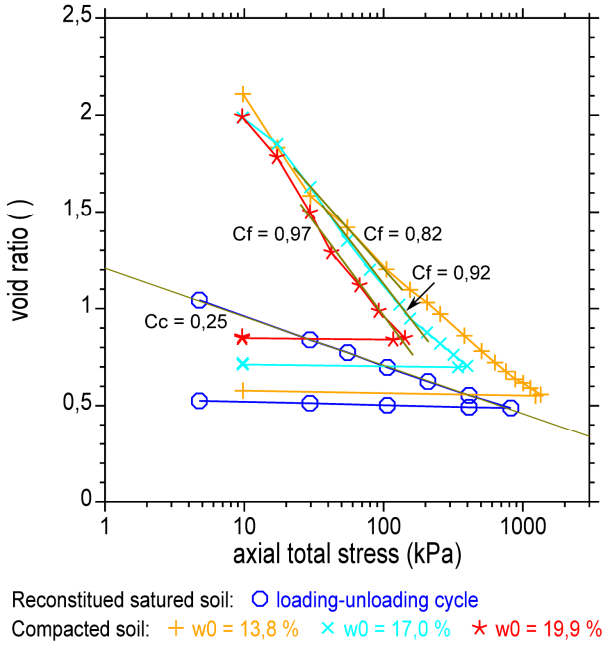

Figure 3. Compaction curves for a clayed silt

The behaviour of Goderville silt was studied for different states of compaction [3]. The program consisted in measuring the mechanical properties at nine state points, then examining the sensitivity of the deformations to the water content [10]. Three static compression curves are shown in the plane ($\log(\sigma_a)$, e) of Figure 3 (as stars). They were derived from different initial water contents (w_0 = 13.8, 17.0 and 19.9%).

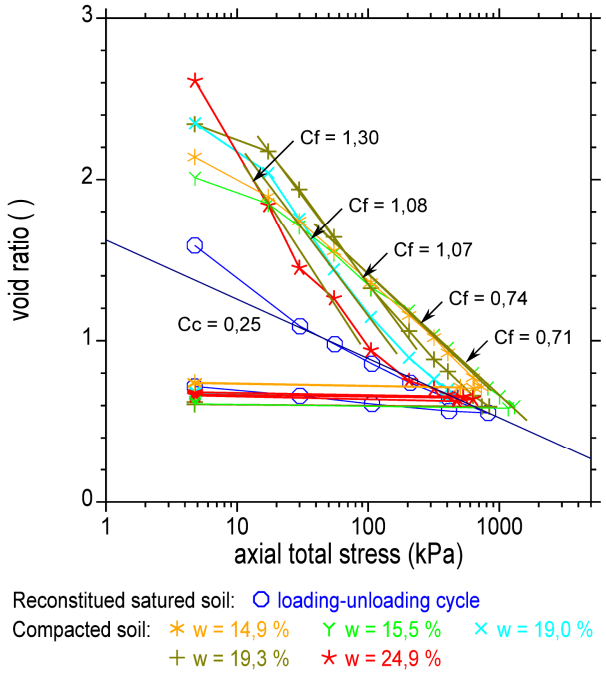

Figure 4. Compaction curves for a plastic clay

The virgin compressibility curve is shown as blue circles (C_c = 0.25). It was achieved by a stepwise oedometer test performed on the soil reconstituted at high water content (w_0 = 58%).

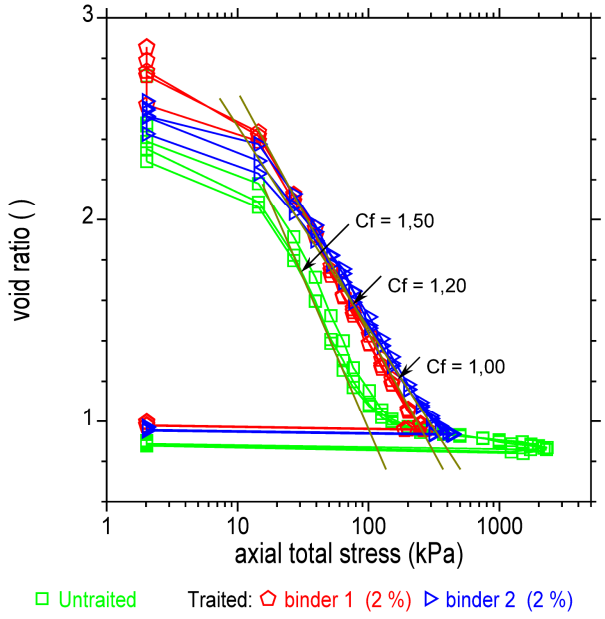

Figure 5. Compaction curves for clayed marl treated with lime or road binder

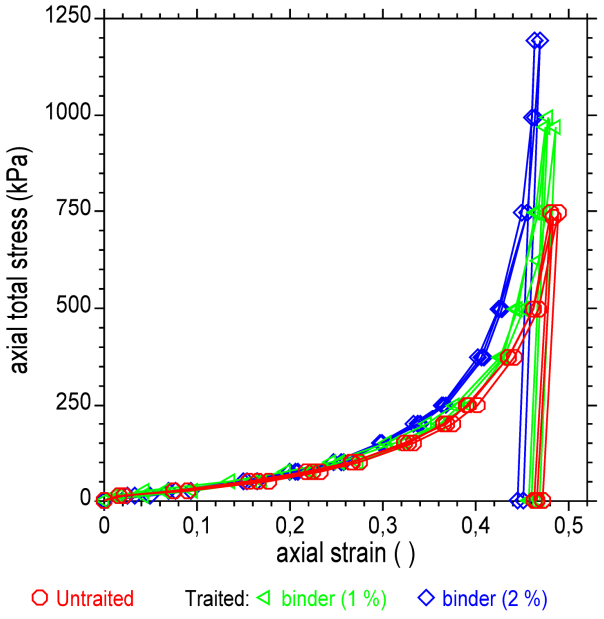

Figure 7. Compaction curves for a weathered marl treated with a road binder

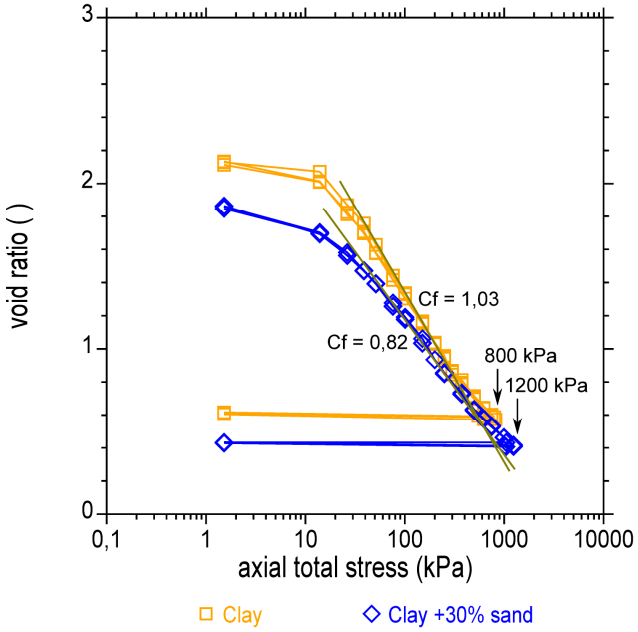

Figure 6. Compaction curves for a plastic clay treated with sand

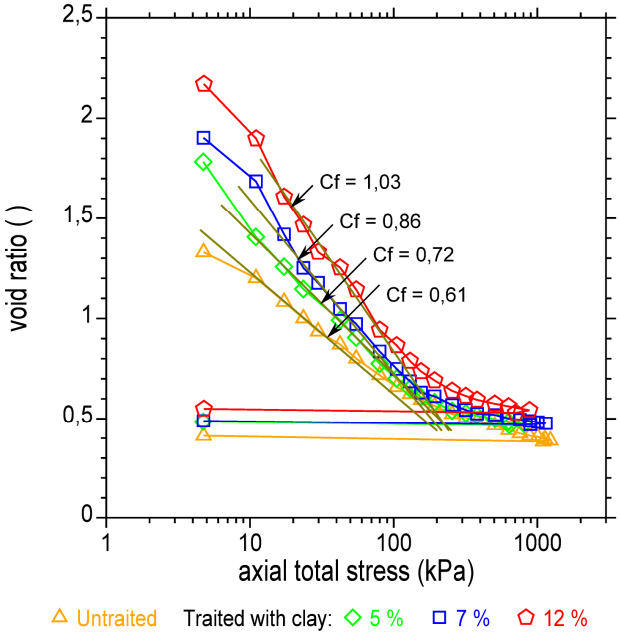

Figure 8. Compaction curves for a sandy-loam treated with bentonite

Three important aspects of static compaction are shown. The compression curves lie above the virgin curve. The maximum slopes C_f of the compression curves increase with increasing moulding water contents (C_f = 0.82, 0.92 and 0.97). At high pressures, the compression curves bend towards the saturated virgin compression curve.

3.2 Example of a plastic clay

The compacted Bavent clay was the object of a semi-scale water transfer experiment [11]. At the same time, the mechanical properties of the clay were measured in the laboratory. Figure 4 shows the oedometer compression curves ($\log(\sigma_a)$, e) of the clay compacted from five initial state points, compared to its virgin compressibility curve ($C_c = 0.25$). The curves gradually shift towards increasing stresses and the slopes C_f decrease. The drier soils require more compaction energy and they are less compressible. The maximum C_f slopes range from 0.7 to 1.3 in this example.

4 Examples for treated soils

4.1 Example of a clayey marl

Figure 5 shows the static compression curves of three triplets of triaxial specimens of a treated or untreated clayey marl. The treatment is carried out using two different binders at a content of 2% (lime or hydraulic road binder). In this example, the compaction of the untreated soil is brought to high pressure in drained condition, which explains the shape of the curve, while the loading of the two treated soils is stopped before this stage. The presence of the binder increases the soil bulking here. Then, the maximum slopes C_f of the treated soils are lower than that of the untreated soil.

4.2 Example of a plastic clay with sand added

Figure 6 compares the compression curves of two sets of triaxial specimens. The plastic clay is treated with sand. The static compaction refers to the Proctor optima established in each of the two cases. The comparison of the compression curves of the clay and the sanded clay mixture confirms the trends already observed during compaction of many different soils. In their bulked state, clay soils are generally looser than silty soils or sandy soils. The compressibility coefficients are higher. The static compaction energy to be provided, which is represented by the axial stress here, is greater in sandy soils. The maximum static stress to be applied is greater in frictional soils. In this sense, higher pressures are required to compact sand-clay mixtures when the proportion of sand increases [6].

4.3 Example of a weathered marl

Figure 7 shows the static compression curves of three triplets of triaxial specimens of a weathered marl. The soil is either untreated or treated with 1% and 2% of a hydraulic road binder. The compression curves are given in linear scales (ε_a, σ_a). It is clear that the energy required to densify the treated soil increases with the binder content. Generally, Proctor compaction works in the same direction, as reported by many authors [12] [13]. The curves in Figure 7 were recorded during the compaction of several triaxial specimens. The curves give an idea of the good repeatability of the static method.

4.4 Example of a sandy loam

Figure 8 shows the static compression curves of four oedometer specimens. The sandy-loam is treated with bentonite in proportions of 0, 5, 7 and 12% of clay. Static compaction refers to the Proctor optima established in each case, which show an increase in w_{OPN} and a reduction in ρ_{dOPN} with increasing clay content. The onset of the static compression curves clearly shows an increase in the initial void ratio e_0 and the maximum slope C_f with increasing bentonite content and the associated water content (C_f ranges from 0.61 to 1.03). However, the compression curves show the difficulty of further densification of the soil as the axial load increases, regardless of the clay content.

5 Discussion

The maximum slopes C_f characterise the compression curves ($\log(\sigma_a)$, e) during the static compaction of fine soils. These maximum slopes were collected from nearly 140 compression curves. They are plotted as a function of the compaction water content w_0

on the graph in figure 9. Each cross represents the compaction of an independent specimen or the compaction of three or six triaxial or oedometer specimens in a given state. The dispersion is large. Nevertheless, a majority of results fall between two lines whose equations are: $C_f = 0.05\ w_0 - 0.125 \pm 0.375$ (w_0 in %).

The particular responses of the treated soils, whose curves are given in Figures 5, 6, 7 and 8, are shown on the graph in Figure 9 (clayey marl, clay with sand, weathered marl, sandy loam). A "0" indicates the response of the untreated soil. The other dots show the progression of the parameters with increasing binder content. The addition of sand (circles) or road binders (squares, triangles) produces an opposite effect to the addition of clay (diamonds).

The maximum slopes C_f are plotted against the void ratio e_f on the graph in Figure 10, where the particular data are also pointed out. A couple of lines frame a majority of responses: $C_f = 0.5\ e_f - 0.60 \pm 0.30$. Within this range the data are sorted into three classes of initial water content ($w_0 < 16\%$; $16\% < w_0 < 20\%$; $20\% < w_0$) and they are ordered in this way to confirm the progression of the pairs (e_f, C_f) with w_0.

Apart from a few points near the origin of the plane (e_f, C_f), which concern sandy soils, the void ratio e_f of the bulked soils vary between 1 and 5 and the maximum slopes C_f vary between 0.1 and 2. Dry soils, which are also the sandiest, are compact and not compressible. In contrast, the wetter soils, which are also the most clayey, are loose and compressible. Similarly, a sorting made on the liquidity limit or the plasticity index shows the same tendency. But these are only trends when the entire data set is examined.

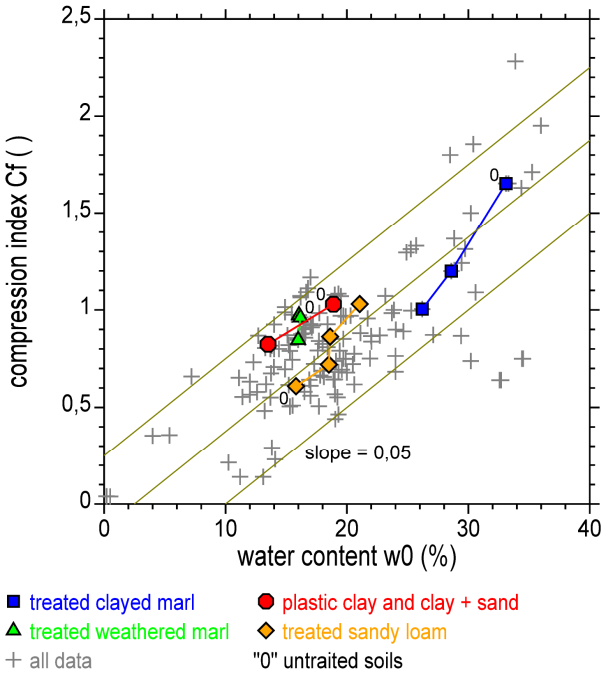

Figure 9. Compression index C_f versus moulding water content w_0

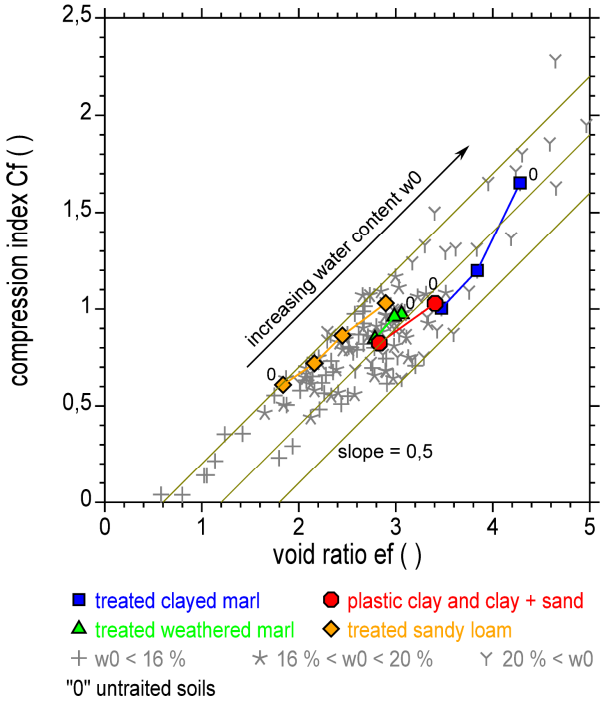

Figure 10. Compression index C_f versus bulked void ratio e_f

6 Conclusions

Static compaction is used to reconstitute fine soil specimens compacted in the laboratory. The static compression curve is recorded to describe the evolution of the volume deformation of the unsaturated bulked soil. A classical semi-logarithmic expression of two parameters (C_f and e_f) is used to describe the soil compressibility.

The individual cases do show that the parameters e_f and C_f increase with the compaction water content and/or with the clay content. Sandy soils or dry clay soils are bulked in denser states. But they are less compressible. Treatment changes the compaction response. Treatment with lime or hydraulic road binders has the effect of reducing e_f and C_f. The addition of sand has a similar effect. On the contrary, treatment with bentonite produces an increase in e_f and C_f.

It is therefore important to record the static compaction curves in the laboratory during the preparatory phases of the mechanical tests, as they reveal a part of the mechanical behaviour of the compacted soils.

7 References

[1] AFNOR (Association Française de Normalisation). Terrassement. Norme NF EN 16907, décembre 2018.

[2] Fleureau J.M., Kheirbek-Saoud S. Variations de résistance des sols compactés avec la pression interstitielle négative. *Rev Fr Géotech*. 1992; **59**: 57‑64.

[3] Ferber V., Auriol J.C., Cui Y.J., Magnan J.P. Comportement des sols fins compactés à l'humidification. Apport d'un modèle de microstructure. *Rev Fr Géotech*. 2008; **122**: 13‑24.

[4] Bell J.R. Compaction energy relationship of cohesive soils. *Transport Res Rec* 1977; **641**: 29–34.

[5] Camapum de Carvalho J., Crispel J.J., Mieussens C., Nardone A. *La reconstitution des éprouvettes en laboratoire. Théorie et pratique opératoire*. Rapport de Recherche des LPC, 145, juin 1987, 54 p.

[6] Moussaï B., Didier G., Atlan Y. Étude d'un matériel de compactage statique et de mesure de la perméabilité des sols fins argileux. *Bull Liaison Lab Ponts Chaussées*. 1993; **188**: 15‑22.

[7] Delage P., Audiguier M., Cui Y.J., Howat D. Microstructure of a compacted silt. *Can Geotech J.* 1996; **33**(1): 150‑158.

[8] Serratrice J.F. Apport expérimental de la méthode de compactage statique des sols au laboratoire. *Rev Fr Géotech*. 2018; **156**, 1.

[9] Mieussens C. *Détermination de la sensibilité des sols aux variations de teneur en eau en laboratoire. Essais à l'oedomètre sur les sols compactés*. Projet de méthode LPC, Rapport du LRPC de Toulouse, 1993; 12 p.

[10] Serratrice J.F. Comportement d'un limon compacté. *Bull Liaison Lab Ponts Chaussées*, 2013; **280-281**: 105-122.

[11] Droniuc N. Étude par la méthode des éléments finis du comportement des remblais en sols fins compactés. *Proceeding of the 18th International Conference on Soil Mechanics and Geotechnical Engineering*, Paris, France, 2013; 1097-1100.

[12] Mitchell J.K., Hooper D.R. Influence of time between mixing and compaction on properties of lime stabilized expansive clay. *High. Res. Board, Bull*. Washington, DC. 1961; **304**: 14-31.

[13] Bell F.G. Lime stabilization of clay minerals and soils. *Engineering geology.* 1996; **42**(4): 223-237.